Structure and Properties of Polyethylene Ionomer Based Nanocomposites

Pablo Santamaría, Jose I. Eguiazábal, Jon Nazábal

Department of Polymer Science and Technology, Institute of Polymer Materials, POLYMAT, Faculty of Chemical Sciences, University of the Basque Country, P. O. Box 1072, 20080 San Sebastián, Spain

Received 2 September 2009; accepted 8 November 2009
DOI 10.1002/app.31771
Published online 14 January 2010 in Wiley InterScience (www.interscience.wiley.com).

ABSTRACT: Li and Zn ionomers of poly(ethylene-*co*-methacrylic acid) were modified by two organically modified montmorillonites by melt mixing. In the nanocomposites (NCs), the increase in the loss tangent main peak temperature indicated a reduction in the mobility of the long-chain segments containing neutralized acid groups. The stack compaction observed by wide-angle X-ray scattering and transmission electron microscopy in the Cloisite 30B based NCs was attributed to the partial degradation of the surfactant and to the irreversible character of the ion-exchange process of the ammonium cation of the surfactant with the Li cation. The considerable dispersion that occurred in the poly(ethylene-*co*-methacrylic acid) zinc salt (PEMA–Zn)/Cloisite 20A (20A) NCs was attributed to the high volume of the surfactant, which reduced undesired interactions between the inorganic clay surface and the ionomer. The ductile nature of the matrix remained in all of the NCs, and the increase in the modulus of elasticity of the PEMA–Zn/20A NCs reached a value five times greater than that of the PEMA–Zn matrix. The results suggest that this ionomer is suitable for use both as a matrix for 20A NCs and as a compatibilizer of polyolefin-based NCs with 20A. © 2010 Wiley Periodicals, Inc. J Appl Polym Sci 116: 2374–2383, 2010

Key words: mechanical properties; melt; nanocomposites; organoclay; polyolefins

INTRODUCTION

Polymer/layered silicate nanocomposites (NCs) have attracted much technological and scientific interest in the recent years because of their ability to improve certain properties, such as the mechanical,[1,2] barrier,[3] and thermal[4,5] properties, of polymeric matrices with very low (<10%) silicate contents. The key to these improvements is the achievement of high levels of dispersion or eventual exfoliation of the clay so that the clay is present in the matrix in the form of platelets with nanometer-scale thicknesses and, consequently, high aspect ratios.[6]

Melt intercalation is the preferred method for dispersing layered clays, but the hydrophilic character of the clay surface usually makes dispersion in polymeric matrices quite difficult. Consequently, organic modification is usually necessary to (1) increase the interlayer distance and (2) lead to favorable interaction with the matrix.[7–9] Once this is achieved, the intercalation of the polymeric matrix inside the interlayer becomes possible; this favors[1] or is the first step[1,10] toward dispersion and eventual exfoliation.

High exfoliation levels were first observed in polyamide 6.[7,11,12] High dispersion levels were obtained without chemical modification of the matrix in matrices such as other polyamides,[13–17] poly(ε-caprolactone),[18–20] poly(ethylene terephthalate) (PET),[9,21,22] poly(trimethylene terephthalate) (PTT),[23] poly(butylene terephthalate) (PBT),[24,25] amorphous copolyester,[26] poly(methyl methacrylate) (PMMA),[27,28] styrene/acrylonitrile copolymer (SAN),[29] and phenoxy.[8] However, in the case of polyolefins, even optimum organic modification did not perform well enough to obtain well-dispersed structures.[30] This was due to the repulsion between the nonpolar polymer and the not fully covered inorganic clay surface.[30,31] Consequently, in addition to the adequate organophilization of the clay, either the addition of a compatibilizer or the chemical modification of the polymer is necessary.[30,32–35] The aim is to lend some polar character to the matrix and thus make adequate the polarities of the polymer and the not fully covered clay surface.

Among strategies for compatibilization and to ameliorate organoclay dispersion in polyolefins, the addition of small amounts of maleic anhydride grafted polyolefin (which is miscible with the unmodified polyolefin) has often been used.[30,34,36,37] Other compatibilizers, such as ethylene/acrylic acid copolymers,[38,39] ethylene/methacrylic acid copolymers,[40] ethylene/vinyl acetate copolymers,[33,41] and oligomers of

Correspondence to: J. I. Eguiazábal (josei.eguiazabal@ehu.es).

Contract grant sponsor: Spanish Ministry of Science and Innovation; contract grant number: MAT 2007-60153.
Contract grant sponsor: Basque Government; contract grant number: GIC07/48-IT-234-07.
Contract grant sponsor: Basque Government (through a grant for the development of this work to P.S.).

oxidized PE,[42–45] have also been used. Recently, ionomers based on copolymers of ethylene and methacrylic acid have also been used as polar compatibilizers in polyolefins.[46,47] The ionomers help dispersion by clearly increasing the polarity of the matrix and, therefore, assisting the matrix–inorganic surface interaction.[46] The relative performance of the ionomers as compatibilizers is under discussion. Thus, the dispersion level of linear low-density polyethylene based NCs with an ionomer and maleic anhydride as a modifier was similar;[46] however, the use of an ionomer in a NC based on polypropylene led to a dispersion increase larger than the dispersion obtained with maleic anhydride grafted polypropylene.[47]

Ionomers have also been used as matrices for NCs. Thus, the effects of the structure of the organic modification of the clay were studied.[48] In NCs based on a sodium ionomer,[48] better shielding of the clay favored exfoliation. This was attributed to the interaction between the ionomer and the alkyl tails of the organoclay and to repulsion of the ionomer by the uncovered minor clay surface. The dispersion level appeared to improve as the neutralization level of the ionomer (sodium) increased.[49] The nature of the neutralizing cation was another relevant parameter. Thus, NCs prepared from sodium and zinc ionomers showed better dispersion and mechanical properties than those prepared with the lithium ionomer.[50] It was proposed that this was a result of the irreversible exchange of quaternary ammonium ions for the very small lithium ions in the galleries of the organically modified montmorillonite (OMMT). This exchange would be reversible in the case of the Zn and Na ions because of their larger size. However, the effects of both the kind of organic modification and the cationic nature on the capacity of ionomers to disperse organoclays are still far from understood.

In this study, NCs based on lithium and zinc ionomers as matrices were obtained in the melt state with two different organoclays. Our aim was to determine (1) the most adequate ionomer/organic modification structure and (2) the effects of the neutralizing cation on the nanostructure and properties of the NCs. With these aims in mind, NCs were obtained by melt extrusion followed by injection molding at organoclay contents ranging from 0 to 7%. The NCs were characterized by wide-angle X-ray diffraction (XRD), transmission electron microscopy (TEM), and dynamic mechanical analysis (DMA), and their properties were measured by means of both tensile and impact tests.

EXPERIMENTAL

Materials

The zinc ionomer, poly(ethylene-*co*-methacrylic acid) zinc salt (PEMA–Zn), used was Surlyn 9970 (DuPont, Wilmington, NC). It had a 15 wt % acid content and a melt flow index of 14 g/10 min at 190°C/2.16 kg and was 50% neutralized. The lithium ionomer was poly(ethylene-*co*-methacrylic acid) lithium salt (PEMA–Li; Aldrich). It had a 15 wt % acid content and a melt flow index of 2.6 g/10 min at 190°C/2.16 kg and was 50% neutralized. Because of the partially polar nature of the ionomer, both a nonpolar and a polar organic modification were used. The organic modifiers of the montmorillonites (MMTs) was a nonpolar two-tailed surfactant, dimethyl bis(hydrogenated tallow) ammonium chloride [Cloisite 20A (20A), Southern Clay Products] and a polar methyl, tallow, bis-2-hydroxyethyl quaternary ammonium surfactant [Cloisite 30B (30B), Southern Clay Products]. Their chemical structures are shown in Figure 1.

Figure 1 Chemical structures of the organic modifiers: (a) 20A and (b) 30B (T = tallow; HT = hydrogenated tallow).

Preparation of the NCs

Drying before processing was performed at 65°C in a vacuum oven for 24 h for both ionomers. The NCs were prepared in a Collin (Ebersberg, Germany) ZK25 corotating twin-screw extruder kneader (screw diameter = 25 mm and length-to-diameter ratio = 30/1) with a barrel temperature (180°C) in the low range proposed by the producer (160–235°C) to minimize degradation. A high screw speed of 200 rpm was used to help exfoliation. The polymers and the organoclays were fed at a constant rate of 1700 g/h. After extrusion, the extrudates were cooled in a water bath and pelletized. To calculate the inorganic content of the OMMTs, calcination of the NCs[8] was not possible because the polymer resulted as a coating of an inorganic residue. Therefore, the MMT/OMMT ratios were obtained by calcination of the pure OMMTs, and the added OMMT contents corresponded, respectively, to 1.50, 3.00, 5.00, and 7.00% MMT. Throughout the article, *X*% for any organoclay refers to the percentage of the inorganic part of the organoclay.

Tensile (ASTM D 638, type IV, thickness = 3.19 mm) and impact (ASTM D 256, thickness = 3.1 mm) specimens were prepared by injection molding in a Battenfeld (Kottingbrunn, Austria) Plus 350/75 reciprocating screw injection molding machine. The melt temperature was 180°C, and the mold temperature was 18°C. The injection speed and pressure

were 11.5 cm^3/s and 900 bar, respectively. After processing, the samples were placed in a desiccator for a minimum of 24 h before testing.

Characterization of the NCs

Calorimetric analyses of the NCs were performed with a PerkinElmer (Norwalk, CT) DSC-7 differential scanning calorimeter. All samples were initially heated from 20 to 120°C at a heating rate of 20°C/min, held at 120°C for 1 min, and subsequently cooled to 20°C at 20°C/min. After the samples were held at 20°C for 1 min, they were reheated as in the first scan. The crystallinity was calculated with a heat of fusion for 100% crystalline polyethylene of 290.4 J/g.[51] DMA was performed with a TA Q800 dynamic mechanical analyzer, which provided the loss tangent (tan δ) versus temperature. The scans were carried out from −50 to 100°C in bending mode at a constant heating rate of 4°C/min and a frequency of 1 Hz.

XRD patterns were recorded in a Philips (Amsterdam, Holland) PW 1729 GXRD X-ray diffractometer at 45 kV and 50 mA with a nickel-filtered Cu Kα radiation source. The scan speed was 0.5°/min.

The TEM samples were ultrathin-sectioned at 60–100 nm with a cryogenic ultramicrotome. The micrographs were obtained in a Philips Tecnai 20 apparatus at an accelerating voltage of 200 kV.

Tensile testing was carried out with an Instron (Bucks, UK) 5569 machine at a crosshead speed of 10 mm/min and at 23 ± 2°C and 50 ± 5% relative humidity. The mechanical properties (tensile strength and ductility, which was measured as the break strain) were determined from the load–displacement curves. Young's modulus was determined by means of an extensometer at a crosshead speed of 1 mm/min. Izod impact tests were carried out on notched specimens with a Ceast (Pianezza, Italy) 6548/000 pendulum. The notches (depth = 2.54 mm and radius = 0.25 mm) were machined after injection molding. A minimum of 5 tensile specimens and 10 impact specimens were tested for each reported value.

RESULTS AND DISCUSSION

Thermal properties

When the NCs were analyzed by differential scanning calorimetry, both the melting temperature (92.3°C for PEMA–Zn and 90.2°C for PEMA–Li) and the crystallinity (14% for PEMA–Zn and 12% for PEMA–Li) were slightly below those of pure polyethylene. Moreover, they did not change when the nanoclay was added; this indicated that the main characteristics of the crystalline phase were similar in the neat ionomer and in the NCs, as has been previously seen in polyethylene matrices.[52,53] A peak appeared in the first heating scan of the ionomers (at 47.3°C for PEMA–Zn and 50.3°C for PEMA–Li), which was indicative of the presence of ionic clusters. However, as its change upon MMT addition was not clear, the results by DMA were those used to examine the phase behavior.

It is known that the main transition of the amorphous phase in ionomers (β′ relaxation) is not the usual glass-transition temperature, and although it is the subject of much controversial discussion, it appears to be related[54,55] to micro-Brownian motions of long-chain segments containing neutralized acid groups. Figure 2 shows the DMA scans of the PEMA–Zn-based NCs with 3 and 5% of both the 20A [Fig. 2(a)] and the 30B nanoclays [Fig. 2(b)] in the temperature range of the peak of the ionomer. The scans of the neat ionomers are also shown as a reference. The increases in $T_{\beta'}$ (temperature of β′ relaxation; main transition of the amorphous phase in ionomers) of PEMA–Li and PEMA–Zn on the addition of the organoclays are collected in Table I. The data of the PEMA–Li NCs are discussed later.

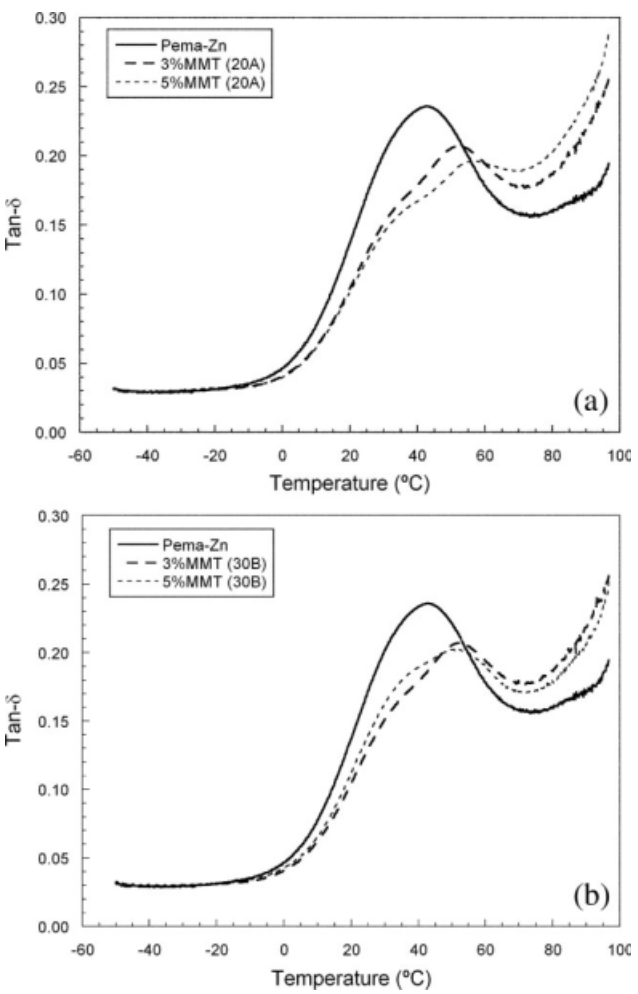

Figure 2 DMA scans of PEMA–Zn-based NCs with organoclays: (a) 20A and (b) 30B.

TABLE I
Increases in $T_{\beta'}$ for PEMA–Zn and PEMA–Li with the Addition of Organoclay

	$\Delta T_{\beta'}$			
	20A		30B	
	3%	5%	3%	5%
PEMA–Zn	9.3	13.3	5.8	8.1
PEMA–Li	2.4	3.5	0.3	1.5

As shown in Figure 2, the peak of the pure PEMA–Zn increased with the addition of 3 and 5 wt % of both organoclays. The higher the nanoclay content was, the higher the increase in the transition temperature was (Table I); this indicated interaction between the neutralized acid groups and the inorganic clay. This interaction should have decreased the mobility of the chain segments associated with the neutralized acid groups and, therefore, shifted the transition in the NCs to higher temperatures. The higher shift in the NCs with the 20A organoclay (Table I) indicated greater interaction, which may have been due to improved dispersion.

In Figure 2(a,b), a shoulder is shown at the left of the main peak of each NC. As shown by the position of the shoulders, the temperature of the peak believed to be causing them appeared to be even below that of the peak of the neat ionomer. Therefore, they must have been due to chain segments associated with the neutralized acid groups that did not interact with the clay and that had higher mobility in the NCs than in the neat ionomer. When we examined the cause of this transition at a low temperature on addition of the organoclay and obviously ruled out the cause being any interaction with the inorganic part of the organoclays, the low temperature transition may well have been due to a migration of the surfactant of the organoclay from the exfoliated layers to the melt polymer during blending. This migration may have been helped by the tendency of both the Zn and Li cations to substitute for the surfactant during melt mixing[50] and is discussed later. As the surfactant was a low-molecular-weight component, it behaved as a plasticizer and increased the mobility of the ionomer, which was not in contact with the clay, and led to a low-temperature transition.

A decrease in the transition temperature upon the addition of nanoclays has not previously been observed to our knowledge in the case of ionomers but has in the case of thermoplastics.[56–58] As the shoulder area was always clearly smaller than that of the main peak, most of the neutralized acid groups appeared to interact with the nanoclay. The higher intensity of the shoulders of Figure 2(b) (with 5% organoclay mainly) indicated that a larger part of the ionomer did not interact with the inorganic clay in the case of the 30B NCs. This suggested poorer dispersion, which was in keeping with the lesser main transition temperature increase displayed by these NCs.

In the PEMA–Li-based NCs, the increases in $T_{\beta'}$ were smaller than those observed in PEMA–Zn (Table I); this indicated poorer interaction and, therefore, dispersion between the Li ionomer and the organoclays. These interpretations were supported by the wide-angle X-ray scattering and TEM results and are discussed in the next section.

Characterization of the nanostructure

The nanostructure of the NCs was studied by both XRD and TEM. The XRD plots of the PEMA–Zn-based NCs with 3 and 5% 20A contents are shown in Figure 3(a), and those of the PEMA–Zn NCs with the 30B nanoclay are shown in Figure 3(b). The

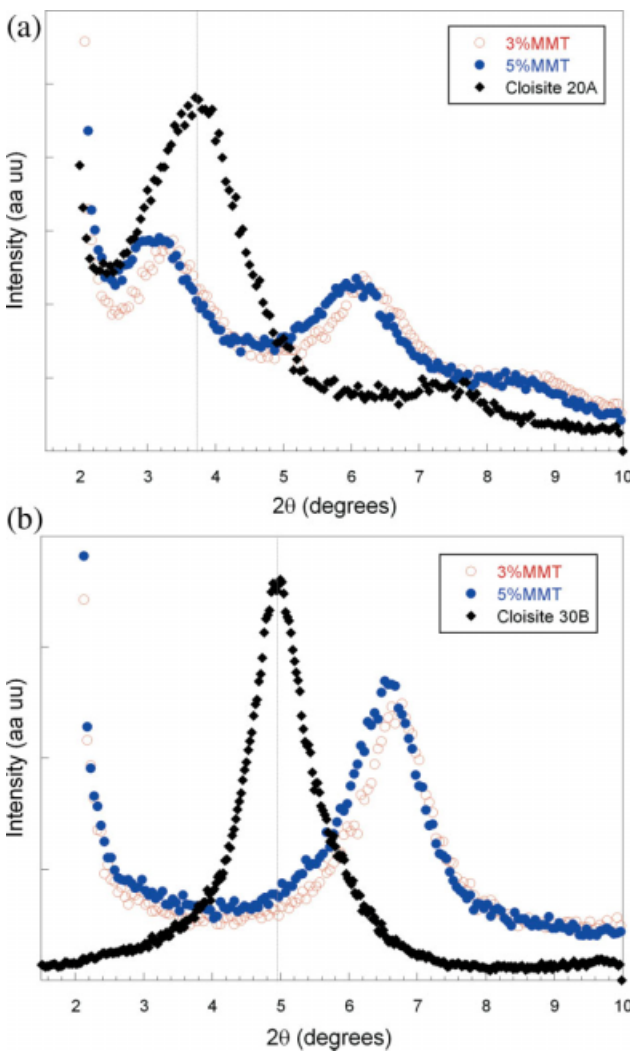

Figure 3 XRD scans of PEMA–Zn-based NCs with organoclays: (a) 20A and (b) 30B. [Color figure can be viewed in the online issue, which is available at www.interscience.wiley.com.]

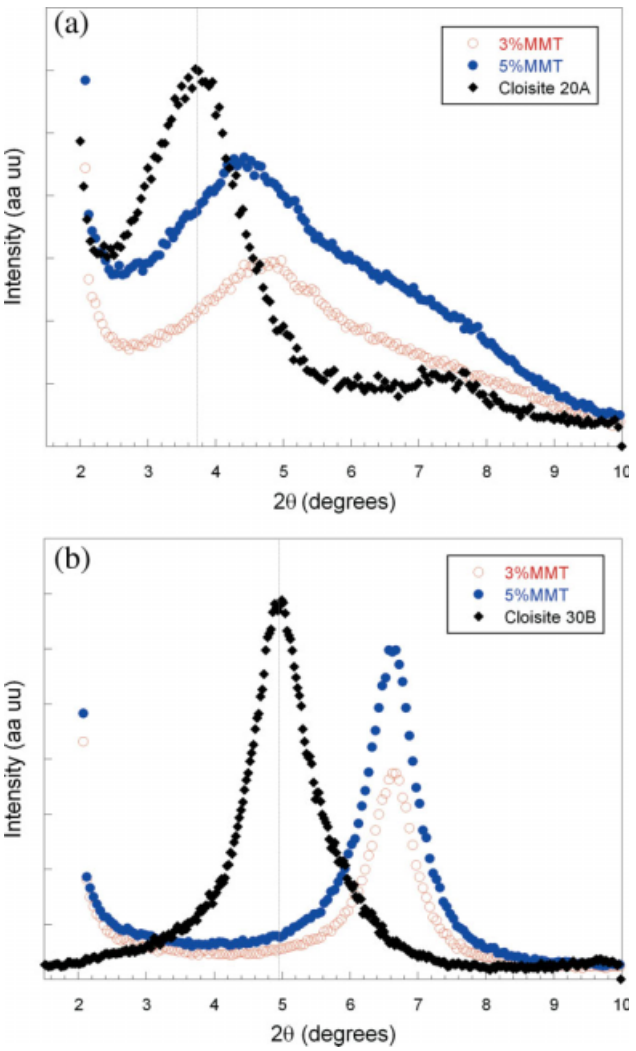

Figure 4 XRD scans of PEMA–Li-based NCs with organoclays: (a) 20A and (b) 30B. [Color figure can be viewed in the online issue, which is available at www.interscience.wiley.com.]

scans of the neat nanoclays are also shown as a reference. The corresponding scans of the PEMA–Li-based NCs are shown in Figure 4(a,b). As shown in Figure 3(a), the diffraction peak of the neat 20A organoclay at $2\theta = 3.73°$ [basal spacing (d_{001}) = 2.36 nm] appeared in the NCs at a lower angle $2\theta = 3.08–3.27°$ (d_{001} = 2.89–2.69 nm); this indicated intercalation of PEMA–Zn into the organoclay layers. The spectrum also showed second- and third-order diffraction peaks, which indicated[8] an ordered morphology of the organoclay as the peaks corresponded to layers located at two or three times d_{001}.

The characteristic peak of the neat 30B organoclay at $2\theta = 4.95°$ (d_{001} = 1.78 nm) in Figure 3(b) shifted after melt mixing to a higher angle of $2\theta = 6.70°$. The correspondent d_{001} (1.31 nm) was lower than that of the neat 30B organoclay; this indicated that the layers compacted upon melt mixing. This indicated degradation of the quaternary ammonium surfactant, as thermal degradation has been seen in its NCs with polyethylene[59] and polystyrene.[60] However, although the processing temperature of this study (180°C) was similar to that of these references (between 180 and 200°C), the peak shifts here were more significant. This suggested the existence of a different degradation mechanism. Literature on the subject suggests that an ion exchange between the quaternary ammonium cation of the surfactant and the metal cations of the ionomers took place.[50] The smaller size of the metal cations compared with the bulky ammonium cations led to a decrease in d_{001}; this explained the compaction observed. The decrease in d_{001} was also helped by the lower thermal stability of the surfactant of the 30B organoclay.[61]

In the scans of the PEMA–Li-based NCs (Fig. 4), the diffraction peaks of the neat organoclays shifted in the 20A NCs to $2\theta = 4.40–4.73°$ (d_{001} = 2.00–1.86 nm) and to $2\theta = 6.63°$ (d_{001} = 1.33 nm) in the 30B NCs. These two d_{001} values were lower than those of the neat organoclays. Thus, because compaction took place in the two organoclays and not only in the 30B organoclay as in the PEMA–Zn-based NCs and, moreover, compaction was stronger in the 30B NCs (lower d_{001} values in the PEMA–Li NC), we deduced that the influence of another parameter besides the degradation of the 30B organoclay must have occurred in the PEMA–Li-based NCs.

During melt mixing, the intercalation process and the ion-exchange reaction took place simultaneously and were competitive processes with regard to d_{001}. It is known[50] that, unlike PEMA–Zn-based NCs, in PEMA–Li-based NCs, the ion exchange has an irreversible character. This irreversibility leads to the ion-exchange process in the PEMA–Li-based NCs being more active than in the PEMA–Zn-based NCs. Thus, in the PEMA–Zn-based NCs, intercalation was the predominant process, but in the case of the PEMA–Li-based NCs, the ion exchange appeared to be the more domineering process. This was the cause of the decrease in d_{001} of the two organoclays shown in Figure 4.

The exfoliated/intercalated relative content of the NCs was studied by TEM. Figure 5(a–d) shows the morphology of the PEMA–Zn-based NCs with 5% of the 20A [Figs. 5(a,b)] and 30B [Figs. 5(c,d)] organoclays at reduced [Fig. 5(a,c)] and large [Fig. 5(b,d)] amplifications. As shown by a comparison of Figure 5(a) and 5(c), the area covered by the clay in the 20A NCs [Fig. 5(a)] was much higher than that shown in Figure 5(c), and consequently, the dispersion in the 20A NCs was much better than in the 30B NCs. This was consistent with the higher increase in the transition temperature of the 20A NCs shown in Figure 2.

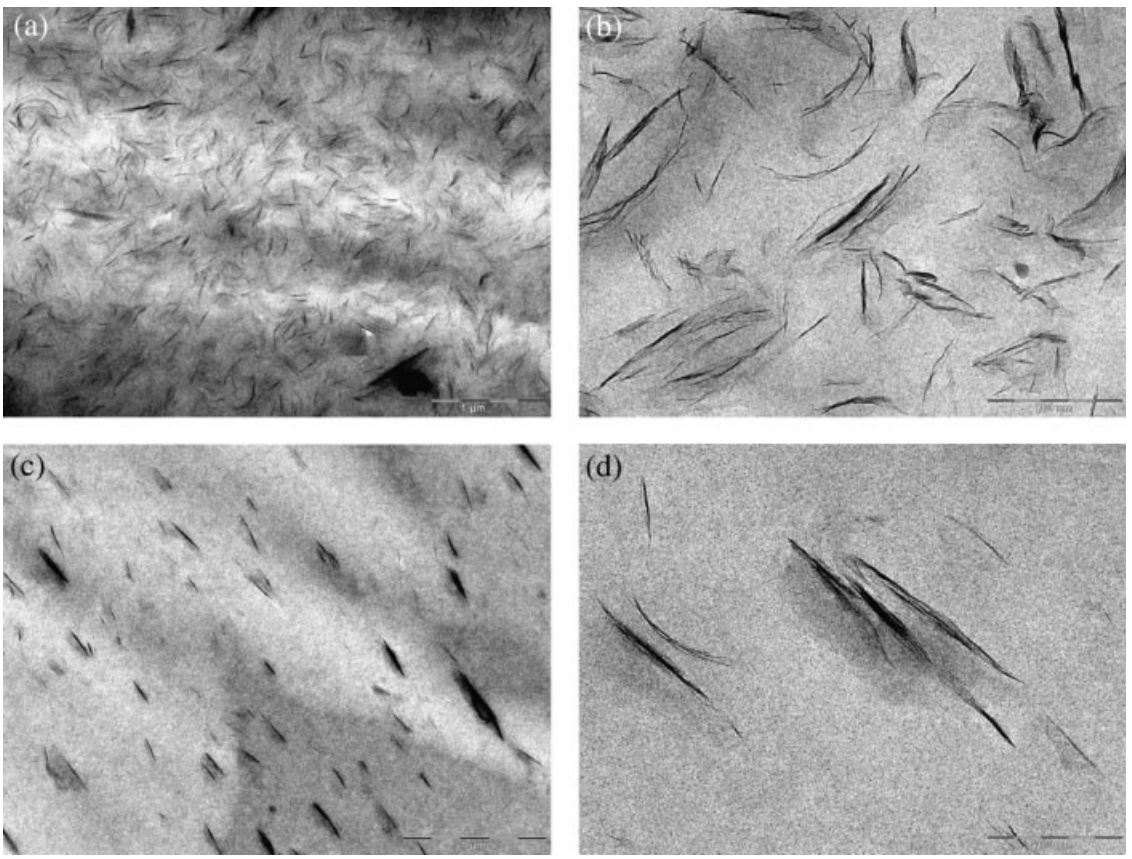

Figure 5 TEM micrographs of PEMA–Zn-based NCs with organoclays with 5 wt % MMT: (a,b) 20A and (c,d) 30B.

In Figure 5(b) (20A organoclay), most of the particles contained a few (2–4) platelets, and some exfoliated platelets were also present. In Figure 5(d) (30B organoclay), although some of the particles contained only 1–2 platelets, most stacks were thicker. Moreover, the single platelets were difficult to differentiate within the particles; this was consistent with the compaction and the low d_{001} (mostly between 1.31 and 1.34 nm) observed previously by wide-angle X-ray scattering.

The occurrence of compaction in the organoclay stacks in the 30B NCs indicated that exfoliation and intercalation were less active here than in the 20A NCs before the degradation of the surfactant occurred. When we examined the reasons for this greater tendency of the 20A NCs to disperse, the main differences in the surfactant structures that appeared to influence dispersion were (1) polarity, which was smaller in 20A, and (2) more importantly, the number of aliphatic chains attached to the nitrogen, which was two in 20A but only one in 30B. The low polarity of 20A should have favored dispersion in the less polar PEMA–Zn matrix; however, the fact that the clay surface was more covered in the 20A NCs because of the higher volume of its substituent (two aliphatic chains) seemed to be the most important of the two. This reduced the undesired interaction between the polymer and the clay surface and led to a more dispersed system.

Figure 6(a–d) shows the TEM micrographs of the PEMA–Li-based 20A [Fig. 6(a,b)] and 30B NCs [Fig. 6(c,d)]. As shown in Figure 6(a,c) and as in the case of the PEMA–Zn-based NCs [Fig. 5(a,c)], the dispersion in the 20A NC was greater than in the 30B NC. As the nature of the cation should not have modified the interaction between the ionomer and the surfactant, this was attributed to the same differences in the surfactant structure as in the case of PEMA–Zn.

Dispersion appeared to be also slightly better in the PEMA–Zn 20A NC [Fig. 5(a,b)] than in the PEMA–Li 20A NC [Fig. 6(a,b)]. The activity of the Li cation substituting for the surfactant was higher[50] than that of the Zn cation because of the irreversible penetration of the Li cation in the interlayer. This higher activity was negative with regard to dispersion because (1) it decreased the polarity of the ionic groups in the polymer and thus reduced its interaction with the part of the clay surface not covered by the surfactant, and (2) more importantly, when the inorganic cation substituted for the surfactant, the interlayer distance decreased and caused an increasing interlayer attraction, which in turn, hindered dispersion.

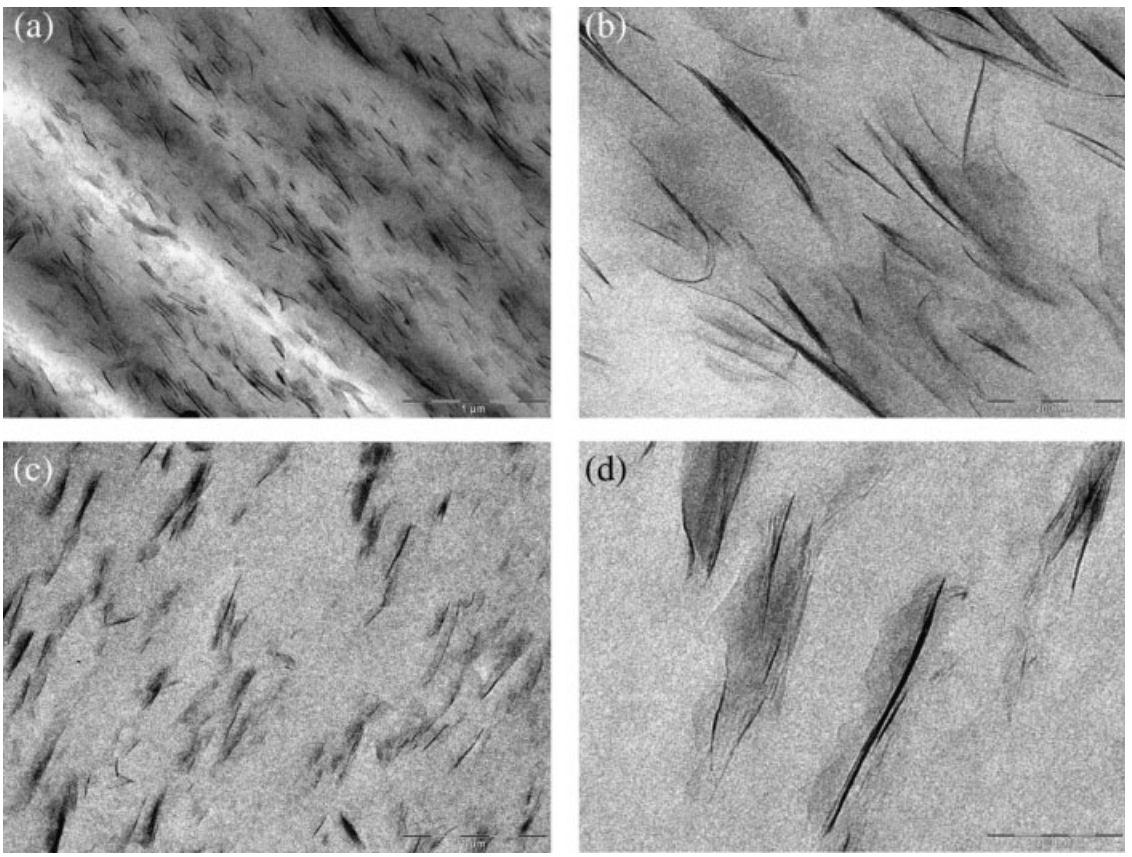

Figure 6 TEM micrographs of PEMA–Li-based NCs with organoclays with 5 wt % MMT: (a,b) 20A and (c,d) 30B.

Mechanical properties

The tensile moduli of the PEMA–Zn and PEMA–Li-based NCs are shown, respectively, in Figure 7(a,b) as a function of both the 20A and 30B content. In all cases, the tensile moduli clearly increased with the organoclay content. In the PEMA–Li-based NCs [Fig. 7(b)], the increases in the 30B NCs were only moderate, but they achieved a 198% increase with respect to the modulus of the matrix after the addition of 7% 20A. Differences in the modulus of the matrix influenced the ability to ameliorate the modulus, but in the PEMA–Zn-based NCs, the addition of 7 wt % 20A led to a huge modulus increase of roughly fivefold that of the ionomer matrix.

These increases in modulus were consistent with the dispersion level of the organoclays observed by TEM. It is known that there is a direct dependence of the modulus of elasticity on dispersion. This is because improved dispersion leads to an increased number of individual platelets and to thinner stacks, that is, to a larger aspect ratio and a high contact area.[6] The existence of a high contact area means that the contribution afforded by stiff reinforcement (which has to bear the externally applied load) becomes more significant; therefore, the modulus increases.

The increases in the modulus observed in this study are collected in Table II, together with those found in the literature for systems with the 20A organoclay based on ionomers and also on both modified and unmodified polyethylene matrices. The low modulus values of all of the reported materials and, consequently, the small differences in modulus among them, make the values significant. As shown, the increases in the moduli of this study were clearly higher than those obtained in both unmodified and modified polyethylene but were also higher than those obtained in other NCs with ionomeric matrices.

Thus, both the TEM and modulus results show that highly dispersed PEMA–Zn ionomer based NCs were obtained with a suitable organoclay such as 20A. This result and the values in Table II also suggest that the PEMA–Zn ionomer may be a suitable compatibilizer for polyethylene-based NCs with 20A, either by direct mixing with the matrix or as a previously produced and widely dispersed master batch.

The ductility (measured as the elongation at break) of the PEMA–Zn and PEMA–Li-based NCs with the two organoclays is plotted against the MMT content in Figure 8. A single plot has been drawn in each figure because the difference between

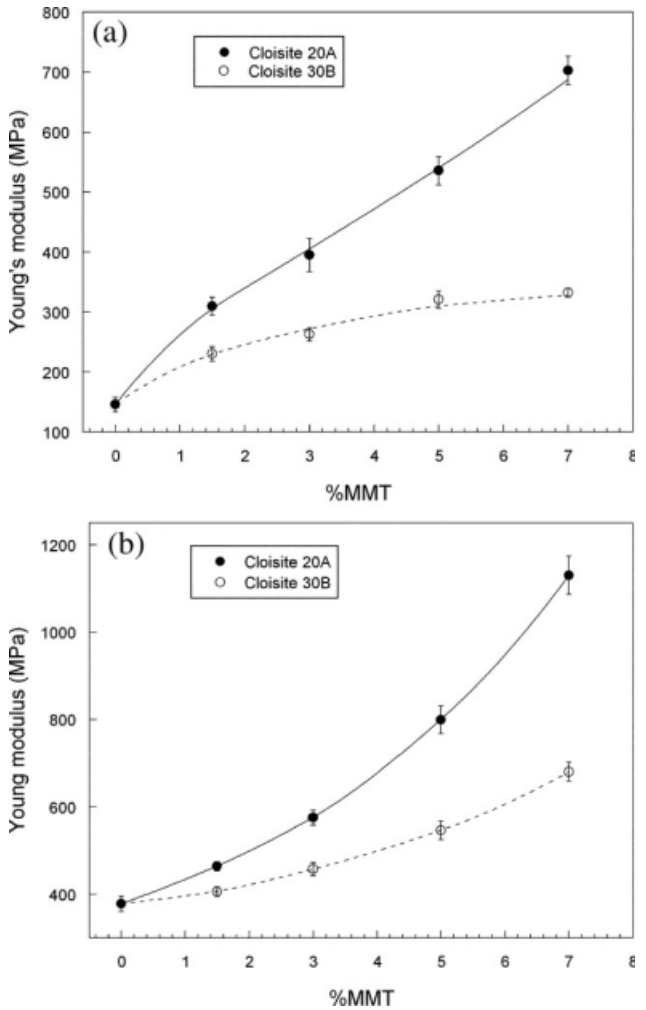

Figure 7 Tensile modulus of (a) PEMA–Zn- and (b) PEMA–Li-based NCs as a function of the MMT content.

the results of the two organoclays was close to the standard deviation. As shown, the ductility of PEMA–Zn-based NCs [Fig. 8(a)] steadily decreased with the clay content, whereas that of the PEMA–Li-based NCs [Fig. 8(b)] remained roughly constant. First, having ruled out the nanostructure, which was rather similar in the two 30B NCs, in an attempt to find any parameter that differentiated the structure of the PEMA–Zn-based NCs from that of the PEMA–Li-based NCs and could have influenced the ductility, we soon realized that the β′ transition (Table I) of the PEMA–Zn increased steadily with the organoclay content. This indicated a decrease in the mobility of the matrix that was consistent with the decrease in ductility shown in Figure 8(a). The similarity also existed in the case of the PEMA–Li NCs, where neither the ductility nor the β′ transition significantly changed. The fact that the two parameters that influenced the β′ transition position (i.e., the interactions with the dispersed clay and the surfactant migration) also influenced the ductility led us to the conclusion that these were the parameters responsible for the observed ductility behavior.

The presence of clay led to an increase in the notched impact strength of all of the NCs (Fig. 9). In the case of these rubberlike materials (neither yielding or cold drawing were observed) and despite the basically different specimens and time and stress conditions in this study, the combination of the plots of the modulus and the elongation at break of Figures 7 and 8, (which are both related to tensile toughness) might suggest a connection with the plot of the notched impact toughness of the four NCs in Figure 9. However, the mechanisms leading to energy dissipation by deformation and fracture of the specimens in the notched impact tests of the polymer NCs are far from understood. Thus, the notched Izod impact strength usually decreases upon clay addition;[62–64] however, increases[8,65] as in this study, and mixed tendencies both in Izod impact strength[48] and in instrumented impact testing[66] have also been reported.

CONCLUSIONS

The addition of organoclays to PEMA–Zn and PEMA–Li ionomers shifted the maximum for the main relaxation of the NCs (due to movements of long-chain segments containing neutralized acid groups) to higher temperatures; this indicated interaction between the neutralized acid groups and the dispersed organoclay. The higher increases in the

TABLE II
Relative Improvements in the Young's Modulus of Various Systems with 5% 20A (Corresponding to 5% MMT)

Reference	Matrix	Compatibilizer	Improvement (%)
30	PE		120[a]
	PE-*g*-MA (0.9 wt % MA)		160[a]
	PE	13% PE-*g*-MA	140[a]
46	PE		8[a]
	PE	18% ionomer	64[a]
	PE	18% PE-*g*-MA	71[a]
67	PE		100
	PEMA (3.9 wt % MA)		120
	PEMA (8.9 wt % MA)		178
50	PEMA–Zn		153
	PEMA–Li		68
	PEMA–Na		118
48	PEMA–Na		113
This study	PEMA–Zn		267
This study	PEMA–Li		111

MA = maleic anhydride; PE = polyethylene; PE-*g*-MA = maleic anhydride grafted polyethylene; PEMA = poly (ethylene-*co*-methacrylic acid).
[a] Interpolated value.

20A NCs were attributed to improved dispersion. The shoulders at the left of the main peaks indicated the presence of neutralized acid groups that did not interact with the clay and probable surfactant migration to the matrix during melt mixing.

Intercalation occurred in the PEMA–Zn-based 20A NCs and compaction occurred in the rest of the systems. The latter was attributed to the degradation of the surfactant of the 30B organoclay and to the irreversible character of the ion-exchange reaction of the Li cation. Compacted stacks coexisted with exfoliated layers, which appeared less often in the PEMA–Li-based 30B NCs. Wide dispersion occurred in the PEMA–Zn-based 20A NCs, where very thin platelets coexisted with fully exfoliated structures. This wide dispersion was mainly attributed to the reduction of the undesired interaction between the polymer and the part of the silicate surface not covered by the high volume surfactant of the 20A organoclay.

The obtained increases in modulus upon organoclay addition were consistent with the dispersion level observed by TEM. Accordingly, moderate increases were observed in the PEMA–Li-based NCs and also in the PEMA–Zn-based 30B NCs. However, the tensile modulus of the PEMA–Zn-based NC with 7% 20A was roughly fivefold that of the matrix; this reflected the wide exfoliation of the 20A organoclay. All NCs remained ductile, and the impact strength increased upon clay addition. Therefore, these results show that the PEMA–Zn ionomer was a matrix that was capable of fully dispersing the 20A organoclay, and we present it as a potential compatibilizer to aid in the dispersion of 20A in polyolefins.

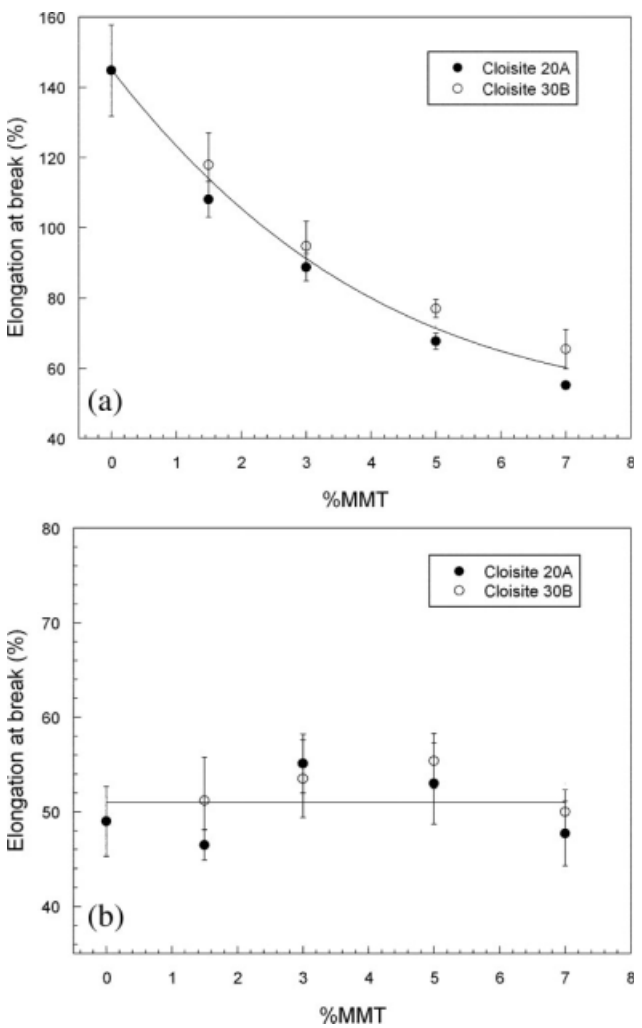

Figure 8 Elongation at break of (a) PEMA–Zn- and (b) PEMA–Li-based NCs as a function of the MMT content.

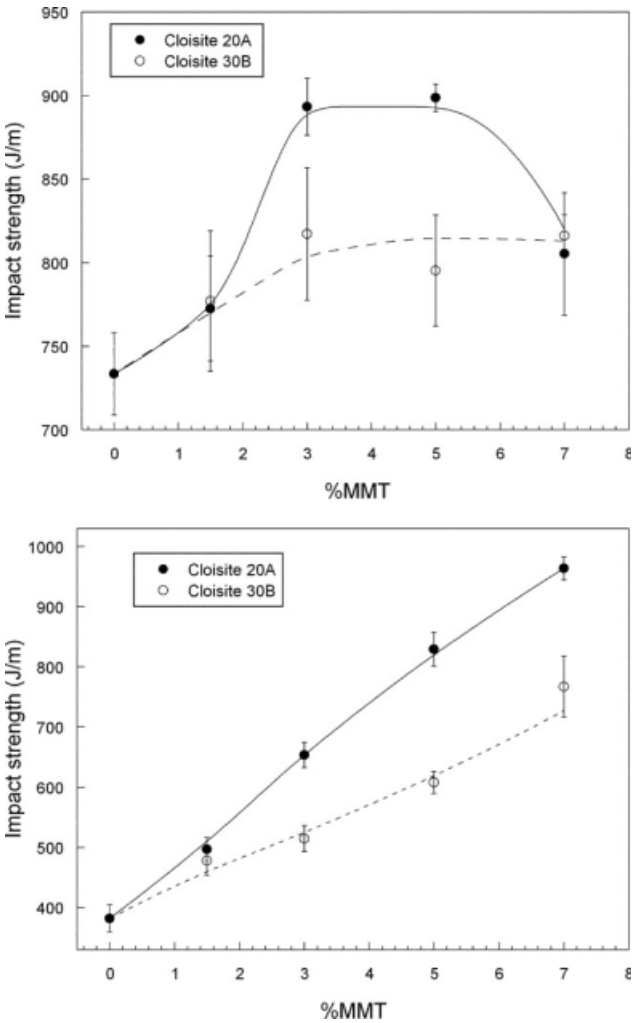

Figure 9 Impact strength of (a) PEMA–Zn- and (b) PEMA–Li-based NCs as a function of the MMT content.

References

1. Clay-Containing Polymeric Nanocomposites; Utracki, L. A., Ed.; Rapra Technology: Shropshire, United Kingdom, 2004; p 1.
2. Fornes, T. D.; Yoon, P. J.; Keskkula, H.; Paul, D. R. Polymer 2001, 42, 9929.
3. Jacquelot, E.; Espuche, E.; Gerard, J. F.; Duchet, J.; Mazabraud, P. J Polym Sci Part B: Polym Phys 2006, 44, 431.

4. Camino, G.; Tartaglione, G.; Frache, A.; Manferti, C.; Costa, G. Polym Degrad Stab 2005, 90, 354.
5. Zhang, J.; Wilkie, C. A. Polym Degrad Stab 2003, 80, 163.
6. Fornes, T. D.; Paul, D. R. Polymer 2003, 44, 4993.
7. Fornes, T. D.; Yoon, P. J.; Hunter, D. L.; Keskkula, H.; Paul, D. R. Polymer 2002, 43, 5915.
8. Gurmendi, U.; Eguiazabal, J. I.; Nazabal, J. Compos Sci Technol 2006, 66, 1221.
9. Gurmendi, U.; Eguiazabal, J. I.; Nazabal, J. Macromol Mater Eng 2007, 292, 169.
10. Tjong, S. C. Mater Sci Eng Rep 2006, 53, 73.
11. Fornes, T. D.; Hunter, D. L.; Paul, D. R. Polymer 2004, 45, 2321.
12. Shah, R. K.; Paul, D. R. Polymer 2004, 45, 2991.
13. Chavarria, F.; Paul, D. R. Polymer 2004, 45, 8501.
14. Han, B.; Ji, G.; Wu, S.; Shen, J. Eur Polym J 2003, 39, 1641.
15. Yu, Z. Z.; Yang, M.; Zhang, Q.; Zhao, C.; Mai, Y. W. J Polym Sci Part B: Polym Phys 2003, 41, 1234.
16. Yoo, Y.; Paul, D. R. Polymer 2008, 49, 3795.
17. Goitisolo, I.; Eguiazábal, J. I.; Nazabal, J. Polym Adv Technol 2009, 20, 1060.
18. Lepoittevin, B.; Devalckenaere, M.; Pantoustier, N.; Alexandre, M.; Kubies, D.; Calberg, C.; Jérôme, R.; Dubois, P. Polymer 2002, 43, 4017.
19. Chen, B.; Evans, J. R. G. Macromolecules 2006, 39, 747.
20. Shibata, M.; Teramoto, N.; Someya, Y.; Tsukao, R. J Appl Polym Sci 2007, 104, 3112.
21. Tsai, T. Y.; Li, C. H.; Chang, C. H.; Cheng, W. H.; Hwang, C. L.; Wu, R. J. Adv Mater 2005, 17, 1769.
22. Davis, C. H.; Mathias, L. J.; Gilman, J. W.; Schiraldi, D. A.; Shields, J. R.; Trulove, P.; Sutto, T. E.; Delong, H. C. J Polym Sci Part B: Polym Phys 2002, 40, 2661.
23. Gurmendi, U.; Eguiazabal, J. I.; Nazabal, J. Eur Polym J 2008, 44, 1686.
24. Li, X.; Kang, T.; Cho, W. J.; Lee, J. K.; Ha, C. S. Macromol Rapid Commun 2001, 22, 1306.
25. Acierno, D.; Scarfato, P.; Amendola, E.; Nocerino, G.; Costa, G. Polym Eng Sci 2004, 44, 1012.
26. González, I.; Eguiazábal, J. I.; Nazábal, J. Macromol Mater Eng 2008, 293, 781.
27. Ratinac, K. R.; Gilbert, R. G.; Ye, L.; Jones, A. S.; Ringer, S. P. Polymer 2006, 47, 6337.
28. Tiwari, R. R.; Natarajan, U. J Appl Polym Sci 2007, 105, 2433.
29. Chu, L. L.; Anderson, S. K.; Harris, J. D.; Beach, M. W.; Morgan, A. B. Polymer 2004, 45, 4051.
30. Hotta, S.; Paul, D. R. Polymer 2004, 45, 7639.
31. Shah, R. K.; Cui, L.; Williams, K. L.; Bauman, B.; Paul, D. R. J Appl Polym Sci 2006, 102, 2980.
32. Hasegawa, N.; Okamoto, H.; Kawasumi, M.; Kato, M.; Tsukigase, A.; Usuki, A. Macromol Mater Eng 2000, 280, 76.
33. Mainil, M.; Alexandre, M.; Monteverde, F.; Dubois, P. J Nanosci Nanotechnol 2006, 6, 337.
34. Wang, K. H.; Choi, M. H.; Koo, C. M.; Choi, Y. S.; Chung, I. J. Polymer 2001, 42, 9819.
35. Pavlidou, S.; Papaspyrides, C. D. Prog Polym Sci 2008, 33, 1119.
36. Zhang, M. Q.; Sundararaj, U. Macromol Mater Eng 2006, 291, 697.
37. Morawiec, J.; Pawlak, A.; Slouf, M.; Galeski, A.; Piorkowska, E.; Krasnikowa, N. Eur Polym J 2005, 41, 1115.
38. Xu, Y.; Fang, Z.; Tong, L. J Appl Polym Sci 2005, 96, 2429.
39. Filippi, S.; Marazzato, C.; Magagnini, P.; Minkova, L.; Dintcheva, N. T.; La Mantia, F. P. Macromol Mater Eng 2006, 291, 1208.
40. Pettarin, V.; Frontini, P. M.; Rodriguez Pita, V. J. R.; Dias, M. L.; Diaz, F. V. Compos A 2008, 39, 1822.
41. Zanetti, M.; Costa, L. Polymer 2004, 45, 4367.
42. Durmus, A.; Kasgoz, A.; Macosko, C. W. Polymer 2007, 48, 4492.
43. Durmus, A.; Woo, M.; Kasgoz, A.; Macosko, C. W.; Tsapatsis, M. Eur Polym J 2007, 43, 3737.
44. Luyt, A. S.; Geethamma, V. G. Polym Test 2007, 26, 461.
45. Geethamma, V. G.; Luyt, A. S. J Nanosci Nanotechnol 2008, 8, 1886.
46. Sanchez-Valdes, S.; Lopez-Quintanilla, M. L.; Ramirez-Vargas, E.; Medellin-Rodriguez, F. J.; Gutierrez-Rodriguez, J. M. Macromol Mater Eng 2006, 291, 128.
47. Liu, H.; Lim, H. T.; Ahn, K. H.; Lee, S. J. J Appl Polym Sci 2007, 104, 4024.
48. Shah, R. K.; Hunter, D. L.; Paul, D. R. Polymer 2005, 46, 2646.
49. Cui, L.; Troeltzsch, C.; Yoon, P. J.; Paul, D. R. Macromolecules 2009, 42, 2599.
50. Shah, R. K.; Paul, D. R. Macromolecules 2006, 39, 3327.
51. Tadano, K.; Hirasawa, E.; Yamamoto, H.; Yano, S. Macromolecules 1989, 22, 226.
52. Truss, R. W.; Yeow, T. K. J Appl Polym Sci 2006, 100, 3044.
53. Peila, R.; Lengvinaite, S.; Malucelli, G.; Priola, A.; Ronchetti, S. J Therm Anal Calorim 2008, 91, 107.
54. Kutsumizu, S.; Tadano, K.; Matsuda, Y.; Goto, M.; Tachino, H.; Hara, H.; Hirasawa, E.; Tagawa, H.; Muroga, Y.; Yano, S. Macromolecules 2000, 33, 9044.
55. Tachino, H.; Hara, H.; Hirasawa, E.; Kutsumizu, S.; Tadano, K.; Yano, S. Macromolecules 1993, 26, 752.
56. Gonzalez, I.; Eguiazabal, J. I.; Nazabal, J. Eur Polym J 2008, 44, 287.
57. Masenelli Varlot, K.; Reynaud, E.; Vigier, G.; Varlet, J. J Polym Sci Part B: Polym Phys 2001, 40, 272.
58. Kim, J. H.; Min Koo, C.; Choi, Y. S.; Wang, K. H.; Chung, I. J. Polymer 2004, 45, 7719.
59. Shah, R. K.; Paul, D. R. Polymer 2006, 47, 4075.
60. Tanoue, S.; Utracki, L. A.; Garcia-Rejon, A.; Tatibouet, J.; Cole, K. C.; Kamal, M. R. Polym Eng Sci 2004, 44, 1046.
61. Cervantes-Uc, J. M.; Cauich-Rodríguez, J. V.; Vázquez Torres, H.; Garfias Mesías, L. F.; Paul, D. R. Thermochim Acta 2007, 457, 92.
62. Zhao, C. G.; Qin, H. L.; Gong, F. L.; Feng, M.; Zhang, S. M.; Yang, M. S. Polym Degrad Stab 2005, 87, 183.
63. Gonzalez, I.; Eguiazabal, J. I.; Nazabal, J. Polym Eng Sci 2006, 46, 864.
64. Stretz, H. A.; Paul, D. R.; Cassidy, P. E. Polymer 2005, 46, 3818.
65. Svoboda, P.; Zeng, C.; Wang, H.; Lee, L. J.; Tomasko, D. L. J Appl Polym Sci 2002, 85, 1562.
66. Yoo, Y.; Shah, R. K.; Paul, D. R. Polymer 2007, 48, 4867.
67. Shah, R. K.; Kim, D. H.; Paul, D. R. Polymer 2007, 48, 1047.